

Screening study of spray solution parameters for depositing cerium-based conversion coatings on Al alloy 2024-T3

Shujiang Geng · Pu Yu · Matthew J. O’Keefe ·
William G. Fahrenholtz · Thomas J. O’Keefe

Received: 22 June 2009 / Accepted: 25 September 2009 / Published online: 11 October 2009
© Springer Science+Business Media B.V. 2009

Abstract Cerium-based conversion coatings were deposited on aluminum alloy 2024-T3 by a spray process using a solution containing cerium chloride, hydrogen peroxide, and gelatin. As deposited coatings were composed of hydrated cerium oxide and were post-treated in a phosphate solution to improve corrosion performance. Coating solution parameters, including the pH (1–2.5), cerium chloride concentration (0.025–0.125 M), and hydrogen peroxide content (0–1.2 M), were varied to investigate the effect(s) of solution parameters on the corrosion performance of the post-treated coatings. Results indicated that thickness of coatings deposited from solutions with different pH values were similar, while coating thickness increased with increasing concentration of cerium chloride and hydrogen peroxide in the solutions. Electrochemical impedance spectroscopy and observations of the surface appearances of the coatings indicated that coatings deposited from solutions with a pH 2, a cerium concentration of 0.1 M, and a hydrogen peroxide concentration of 0.8 M exhibited the best corrosion resistance.

Keywords Al 2024-T3 · Cerium conversion coating · Solution parameters · Corrosion · EIS

1 Introduction

Alloying additions are used to improve the mechanical behavior of aluminum alloys. For aluminum alloy 2024-T3, copper additions improve the strength due to the formation of copper-rich intermetallic compounds (IMCs) [1]. However, IMCs promote pitting corrosion due to the galvanic couples that form between the copper-rich intermetallics and the copper-depleted matrix. Corrosion of copper-containing Al alloys such as 2024-T3 is thought to be enhanced compared to pure Al by the cathodic activity of the intermetallic particles, which serve as preferential sites for the reduction of oxygen [2]. In applications that lead to exposure to aggressive species such as halides, Al alloy 2024-T3 is often coated for protection against corrosion. Conversion coatings are applied directly to aluminum alloy surfaces to improve corrosion resistance and the adhesion of subsequent organic layers such as primers. Chromate conversion coatings (CrCCs) have been widely used to protect metallic materials including Al alloy 2024-T3 [3–9]. However, health and environmental concerns about the toxic and carcinogenic nature of chromates have recently led to increased government regulation, which has resulted in a significant increase in the life-cycle costs associated with depositing and maintaining systems protected with chromated coatings. As a consequence, efforts are underway to develop environmentally acceptable replacements of chromated coatings.

Over the past 20 years, cerium-based conversion coatings (CeCCs) have been investigated for the corrosion protection of high strength aluminum alloys [10–17]. These coatings are among the most promising alternatives to chromates because they are environmentally benign and capable of providing significant corrosion protection [14]. CeCCs have been deposited on Al alloy 2024-T3 using

S. Geng · P. Yu · M. J. O’Keefe (✉) · W. G. Fahrenholtz ·
T. J. O’Keefe
Department of Materials Science and Engineering, Graduate
Center for Materials Research, Missouri University of Science
and Technology, Rolla, MO 65409, USA
e-mail: mjokeefe@mst.edu

immersion methods [18–20]. Recently, CeCCs have also been deposited on Al alloy 2024-T3 using a spray process that employs a water-based solution containing cerium chloride and hydrogen peroxide [21–26]. Previous research has shown that processing parameters of CeCCs have a large impact on the corrosion resistance. While parameters such as surface preparation [15, 16, 25], gelatin concentration in the spray solution [24], post treatment [15, 16], and coating deposition method [17] have been investigated and optimized, a thorough study on the optimum concentration of cerium chloride and hydrogen peroxide along with the pH of the coating solution is lacking. A study on such parameters is especially important as studies have shown the critical roles that hydrogen peroxide [27] and pH [28] can have on the deposition or precipitation of cerium species.

In the present article, CeCCs were deposited on Al alloy 2024-T3 by means of a spray process. The effects of variations in pH, concentration of cerium chloride, and concentration of hydrogen peroxide in the spray solution were studied. The electrochemical behavior of the coatings was investigated and the results were analyzed with respect to the processing parameters.

2 Experimental

Aluminum alloy 2024-T3 panels (nominal composition in weight percent: 0.5% Si, 0.5% Fe, 3.8–4.9% Cu, 0.3–0.9% Mn, 1.2–1.8% Mg, 0.1% Cr, 0.25% Zn, 0.15% Ti, and the balance Al) with dimensions of 15.2 cm × 7.6 cm × 0.1 cm (6 in × 3 in × 0.04 in) were chosen for these experiments as it and 7075-T6 are common high strength aluminum alloys in which corrosion resistant coatings are tested on. Prior to coating, panels underwent a series of surface preparation processes. Substrates were first rinsed with acetone then thoroughly rinsed with deionized water. Next, panels were immersed in a 1 wt% H₂SO₄ solution for 5 min at 50 °C, followed by thorough rinsing with deionized water. Panels were then treated in a 5 wt% solution of alkaline cleaner (4215 NCLT, Turco Products) for 5 min with agitation at 55 °C, followed by thorough rinsing with deionized water.

Conversion coatings were deposited at room temperature by a spray deposition method. The coating was deposited from a 250 mL water solution with concentrations of CeCl₃·7H₂O (99.9% Alfa Aesar, Ward Hill, MA) ranging from 0.025 to 0.125 M, concentrations of hydrogen peroxide (30 wt% solution, Fisher Scientific, Fairlawn, NJ) ranging from 0 to 1.2 M, and 0.8 g of a water soluble gelatin (SPH [Derived from pig skin], Rousselot). The pH of the spray solution was adjusted to between 1.0 and 2.5 with HCl. Panels were kept upright at an angle of

60° to the horizontal so that the solution remained in contact with the substrate as it flowed down and off the surface. A detail spray gun (Model IFS55, Campbell Hausfeld, Harrison, OH) was used to spray the solution onto the panels. The gun was attached to a filtered air supply maintained at a pressure of 25 psi. After a uniform layer of solution was applied to the panel surface, the panel was allowed to drain for 1 min before more solution was sprayed onto it. The spray-drain cycle was repeated five times. After deposition, the panels were rinsed with deionized water and post-treated by immersion for 5 min at 85 °C in a solution which was a mixture of 2.5 wt% Na₃PO₄·12H₂O in deionized water adjusted to pH 4.5 with phosphoric acid. Substrates were kept wet (non-breaking water film) between each step of the cleaning/coating/post-treatment process. Panels with CeCCs were stored at room temperature in the laboratory for at least 24 h before characterization or performance evaluation.

Scanning electron microscopy (SEM; Hitachi S-4700) with energy dispersive X-ray spectroscopy (EDS; Phoenix System) was used to characterize the surface morphologies and compositions of CeCCs before and after corrosion testing. Auger electron spectroscopy (AES; Perkin-Elmer 545) depth profiling was used to measure coating thickness. Coating thicknesses were judged by the point where the Ce and Al lines crossed [22, 23]. A sputter rate of 9 nm/min was assumed based on results from a Ta₂O₅ standard.

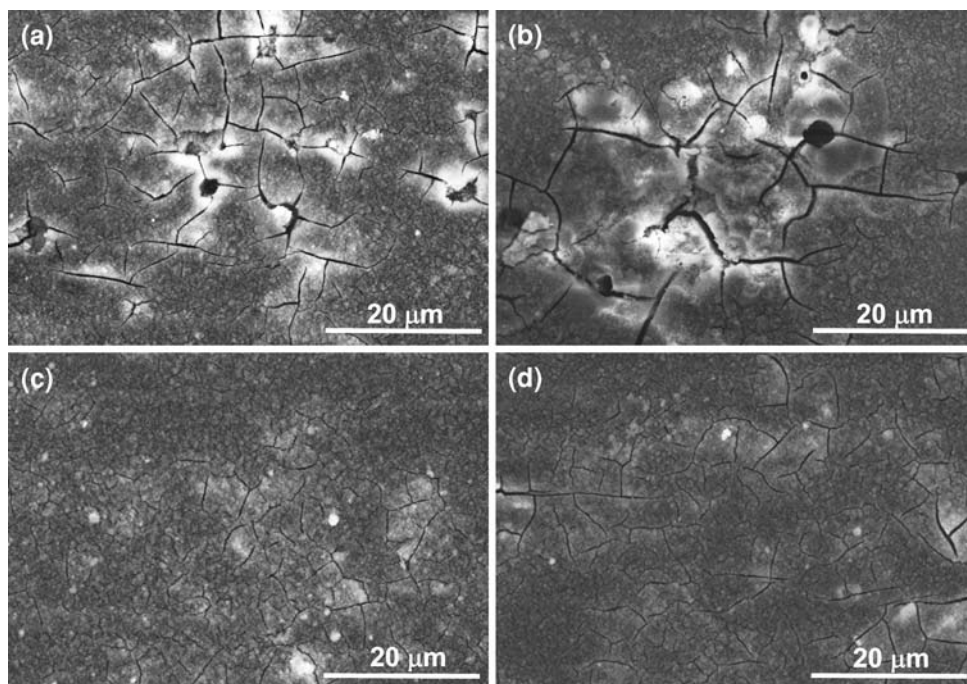
Electrochemical impedance spectroscopy (EIS) was carried out at open circuit potential with an amplitude of 10 mV in the frequency range from 10⁵ to 10⁻² Hz. Measurements were made after immersion times ranging from 1 to 5 h. All experiments were conducted with a frequency response analyzer (Schlumberger SI 1255 HF) and a potentiostat/galvanostat (EG&G Princeton Applied Research Model 273A). The electrochemical cell was a 250 mL jacketed beaker maintained at 30 °C. The cell was filled with prohesion solution, which consisted of 0.35 wt% (NH₄)₂SO₄ and 0.05 wt% NaCl in deionized water. The exposed area of the working electrode was 6.4 cm². A saturated calomel electrode (SCE) was used as the reference electrode (RE) and Pt mesh with an area of 12 cm² was used as the counter electrode.

3 Results and discussion

3.1 Effect of pH in the spray solution

Figure 1 shows the surface morphologies of CeCCs that were prepared from spray solutions with pH values adjusted to 1.0, 1.5, 2.0, and 2.5. The concentrations of Ce³⁺ and H₂O₂ in this spray solution were 0.1 and 0.8 M, respectively. Cracks and holes were visible in the coatings

Fig. 1 SEM surface morphologies of CeCCs on Al alloy 2024-T3 deposited by the spray processes from solutions with pH values of 1.0 (a), 1.5 (b), 2.0 (c), and 2.5 (d)



deposited from solutions with pH 1.0 and 1.5. Analysis by EDS indicated that less Ce and more Al were detected inside the areas that appeared to be holes. The measured Ce content inside the holes was ~ 6 wt%, which was lower than that in areas with a uniform coating, which was ~ 30 wt%. This indicates that a thin coating may be present inside the holes. Coatings deposited from solutions with higher pH values (2.0 and 2.5) appeared to be more uniform, had smaller cracks, and had a measured Ce concentration of ~ 30 wt%. Previous research showed that strength of the Ce signal measured by EDS was a qualitative indication of CeCC thickness, with thicker coatings having a stronger Ce signal [29]. Analysis by AES depth profiling as part of the present investigation revealed that a coating deposited from the solution with a pH of 2.0 was ~ 350 nm thick. EDS was used to make multiple measurements of the same coating, an average Ce concentration of ~ 30 wt% was detected. The average amount of Ce detected by EDS in the uniform areas of the coatings shown in Fig. 2 was around 30 wt%, indicating the thicknesses of the coatings deposited from solutions with different pH values were similar. Based on these observations and the thickness of ~ 350 nm measured by AES for the coating deposited from the solution with a pH of 2.0, coating thickness was ~ 350 nm for all solution pH values. The difference was that coatings deposited from solutions with pH 2.0 and 2.5 had fewer cracks and other defects.

Figure 3 shows Nyquist plots for coatings deposited from solutions with different pH values. The measurements were made after immersion in prohesion solution at 30 °C for 1, 3, and 5 h. The EIS results indicated that the coatings

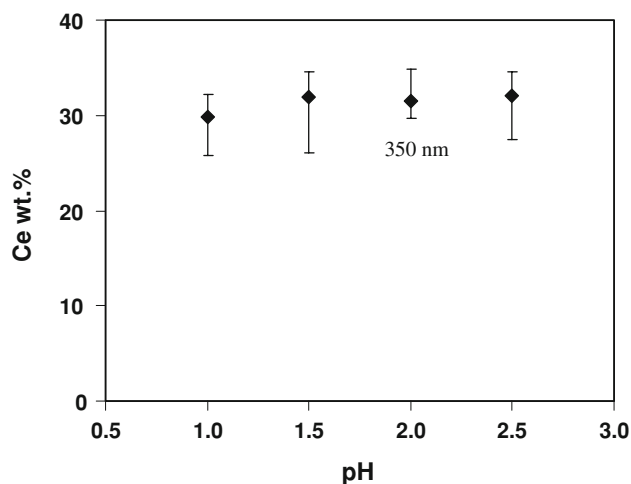


Fig. 2 Ce concentrations detected by EDS for spray deposited CeCCs on Al 2024-T3 with the corresponding thickness of the coating deposited from a solution with a pH of 2.0 as measured by AES depth profiling

deposited from solutions with pH 2.0 and 2.5 had higher impedance values than coatings deposited from solutions with pH 1.0 and 1.5 after 1, 3, and 5 h of testing. For coatings deposited from solutions with pH 2.0 and 2.5, the impedances were $\sim 1.0 \times 10^5 \Omega \text{ cm}^2$, $6.0 \times 10^4 \Omega \text{ cm}^2$, and $3.5 \times 10^4 \Omega \text{ cm}^2$, after 1, 3, and 5 h, respectively. In contrast, the coatings deposited from solutions with pH 1.0 and 1.5 had lower impedance values of $5.0 \times 10^4 \Omega \text{ cm}^2$, $1.5 \times 10^4 \Omega \text{ cm}^2$, and $1.0 \times 10^4 \Omega \text{ cm}^2$ after 1, 3, and 5 h of immersion. It should be noted that the impedance of the coating deposited from the solution with pH = 2.0 was

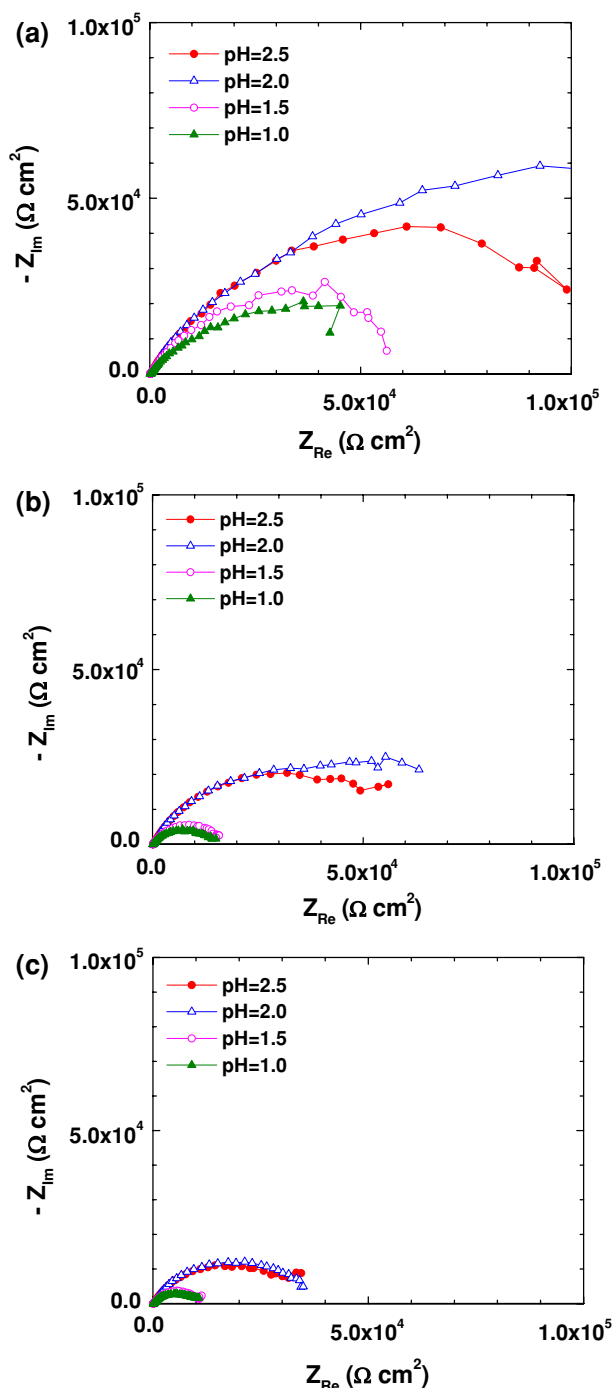


Fig. 3 Nyquist diagrams for CeCCs on Al alloy 2024-T3 deposited from spray solutions with different pH values after immersion in prohesion solution at 30 °C for 1.0 h (a), 3.0 h (b), and 5.0 h (c)

initially higher than the impedance of the pH 2.5 coating, but after 5 h the values were equivalent, likely due to some aspect of the surface chemistry of the pH 2.0 coating that was not in equilibrium after 1 h but became so after 3–5 h.

The surface appearances of coatings deposited from solutions with different pH values were observed after 5 h of immersion in the EIS test solution. In particular, the

formation of white reaction products from pitting corrosion was noted. The corrosion behavior of the coating deposited from the solution with pH 1.0 was similar to that of the coating deposited from solution with pH 1.5. Both of these coatings had more extensive pitting corrosion than the coatings deposited from solutions with pH 2.0 and 2.5. The increased corrosion of the coatings deposited from solutions with pH 1.0 or 1.5 was most likely due to the larger number of holes and larger cracks in these coatings. The surface appearances of the coatings after 5 h of immersion were consistent with the EIS data as shown in Fig. 3c. Coatings with higher impedance (i.e., better corrosion resistance) had fewer pits (i.e., less corrosion) after testing than coatings with measurably lower impedance.

Although the pH of the spray solution had no measurable effect on the coating thickness, the pH did affect the coating uniformity and, therefore, the corrosion performance of the coatings. The impedance and pitting corrosion resistance of the coatings deposited from the solutions with higher pH values (2.0 and 2.5) was better than that of the coatings deposited from the solutions with lower pH values (1.0 and 1.5). The solutions with pH values lower than 2.0 were chemically aggressive, leading to the formation of defects in the coatings, which promoted pitting corrosion. It should be noted that solutions with pH values higher than 2.5 were not stable and cerium hydroxide/oxide precipitated spontaneously in solution the presence of H_2O_2 . Therefore, coatings could not be produced from solutions with pH values greater than 2.5.

3.2 Effect of Ce^{3+} concentration in the spray solution

The cerium concentration, $[\text{Ce}^{3+}]$ in the spray solutions was varied from 0.025 to 0.125 M. In all of the solutions, the concentration of H_2O_2 was maintained at 0.8 M. Based on the pH studies, the pH of solutions was adjusted to 2.0 using dilute HCl. As seen in Fig. 4, coatings from solutions with lower Ce^{3+} concentrations were not uniform. Large, localized nodules were observed on the surfaces of coatings deposited from solutions with $[\text{Ce}^{3+}]$ of 0.025 and 0.05 M (Fig. 4a, b). For coatings deposited from solutions with $[\text{Ce}^{3+}]$ of 0.075 and 0.1 M, more uniform coatings were deposited, as shown in Fig. 4c, d. In the case of coatings deposited from the solution with a $[\text{Ce}^{3+}]$ of 0.125 M, larger and wider cracks were observed (Fig. 5e). The amounts of Ce detected in the coatings by EDS increased with increasing concentration of Ce^{3+} in the spray solution. Similarly, the thickness of the coatings measured by AES depth profiling analysis increased with increasing concentration of Ce^{3+} as indicated in Fig. 5. Coating thickness increased from ~ 150 nm for the lowest cerium concentration (0.025 M) to ~ 350 nm for cerium concentrations of 0.100 and 0.125 M. After increasing with

Fig. 4 Surface morphologies of CeCCs on Al 2024-T3 deposited from spray solutions with $[Ce^{3+}]$ of 0.025 M (a), 0.05 M (b), 0.075 M (c), 0.1 M (d), and 0.125 M (e)

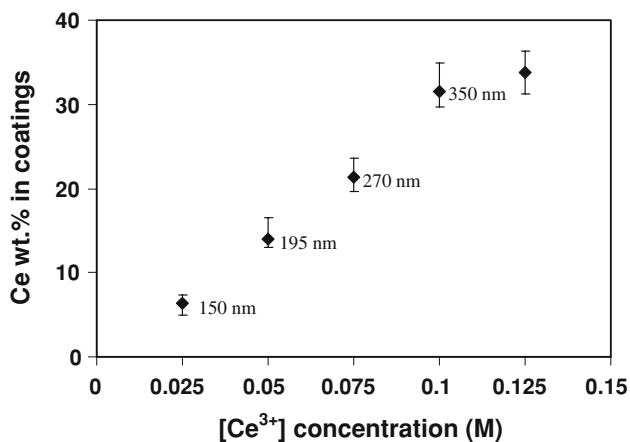
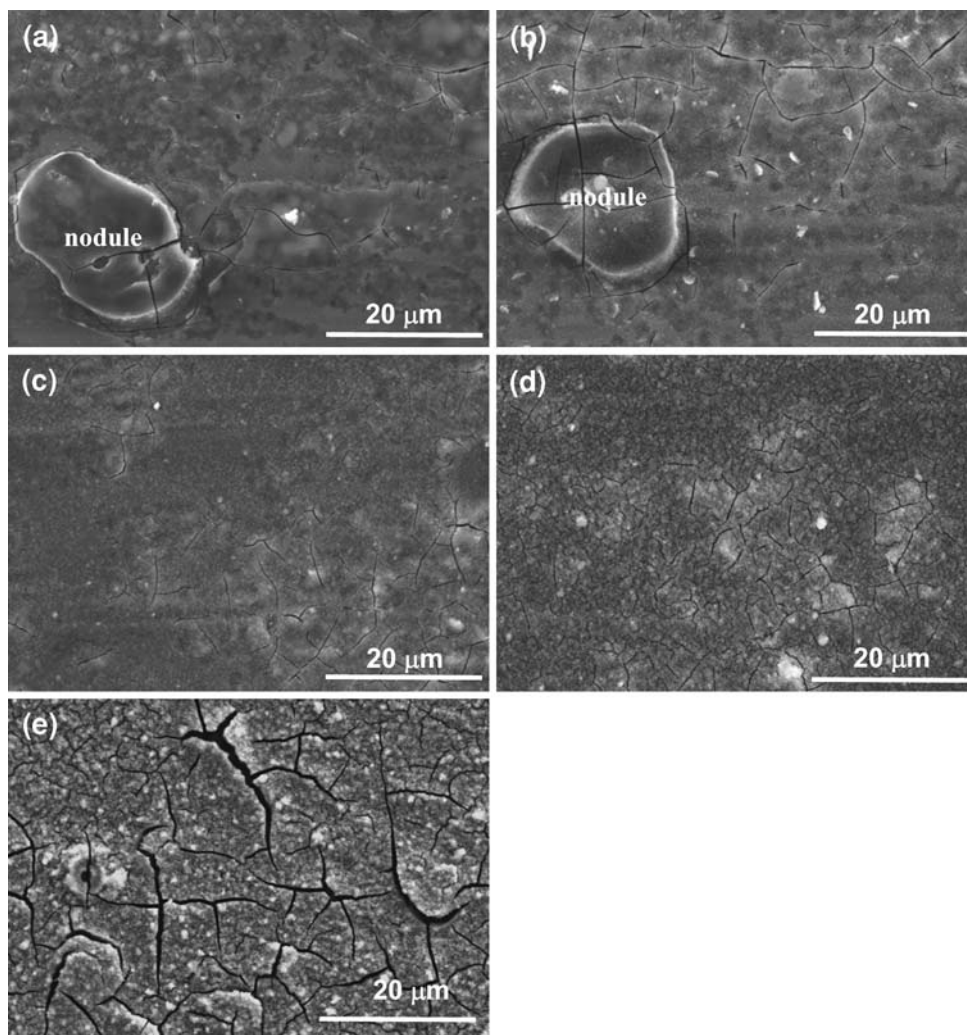


Fig. 5 The amount of Ce detected in CeCCs by EDS as a function of the pH of the spray solution along with corresponding thicknesses measured by AES depth profiling analysis

increasing concentration of Ce^{3+} initially, coating thickness appears to level off above 0.100 M. This change in behavior could indicate that the coating deposition rate was

limited by availability of Ce ions at lower concentrations, which may be related to transport of Ce^{3+} from the bulk solution to the near-surface region where Ce species precipitate and form the coating. [27] In contrast, Ce^{3+} concentrations of 0.100 M or higher may be sufficient to overcome this limitation and lead to coating deposition rates that depended on some other factor such as the rate of precipitation of cerium species.

Nyquist plots for the coatings deposited from solutions with different concentrations of Ce^{3+} after immersion for 1, 3 and 5 h in prohesion at 30 °C are shown in Fig. 6. The impedance values after 1 h of testing indicated that coatings deposited from solutions with Ce^{3+} concentrations of 0.075–0.125 M had impedance values of more than $1.0 \times 10^5 \Omega cm^2$ while coatings deposited from solutions with Ce^{3+} concentrations of 0.025 and 0.05 M had impedances less than $5.0 \times 10^4 \Omega cm^2$. After 3 and 5 h of immersion in the test solution, the impedance values of the coatings deposited from the solutions with Ce^{3+} concentrations of 0.1 M (3 h, $6.5 \times 10^4 \Omega cm^2$; 5 h, $3.5 \times 10^4 \Omega cm^2$) and 0.125 M (3 h, $5.5 \times 10^4 \Omega cm^2$; 5 h, $4.5 \times$

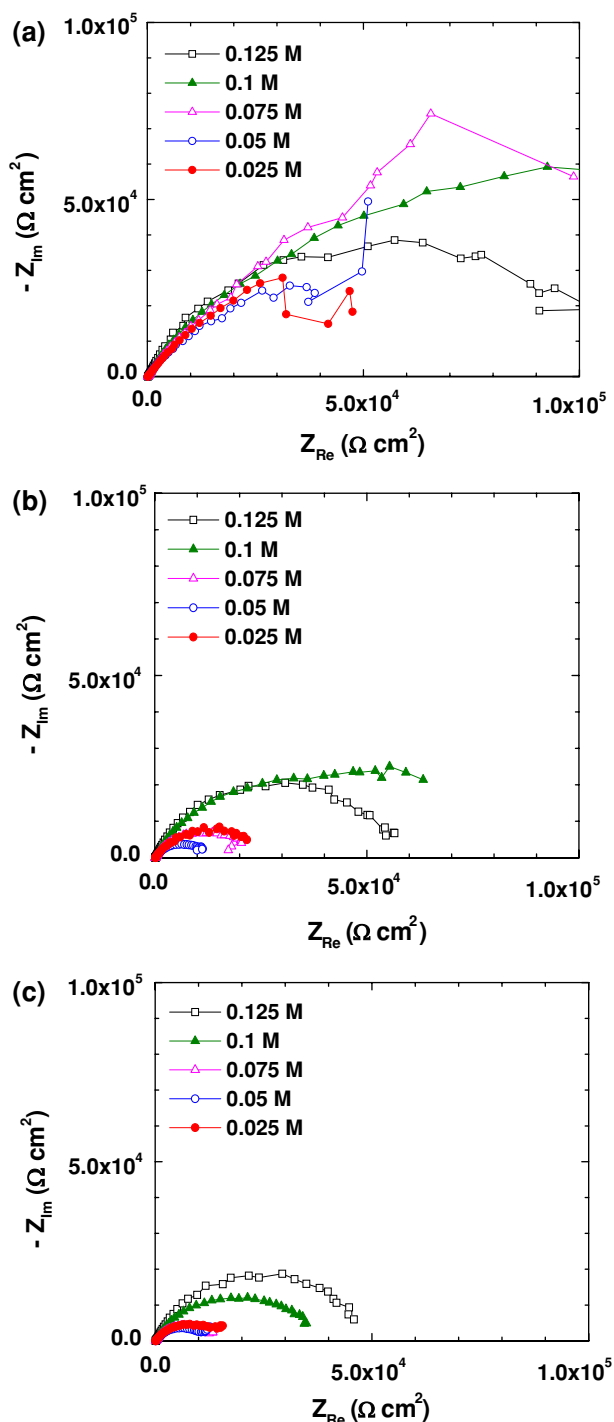


Fig. 6 Nyquist diagrams for CeCCs on Al alloy 2024-T3 deposited from solutions with different of Ce^{3+} concentrations after immersion in prohesion solution at 30 °C for 1.0 h (a), 3.0 h (b), and 5.0 h (c)

$10^4 \Omega \text{ cm}^2$) were higher than those of the other three coatings deposited from solutions with lower Ce^{3+} concentrations ($<2.5 \times 10^4 \Omega \text{ cm}^2$ for all samples). The impedance of the coating deposited from the solution with a Ce^{3+} concentration of 0.1 M was higher than that of the

coating deposited from solution with a Ce^{3+} concentration of 0.125 M after 1 and 3 h of immersion in the test solution. However, the coatings deposited from solutions with Ce^{3+} concentration of 0.1 and 0.125 M had similar impedance values, around $4.0 \times 10^4 \Omega \text{ cm}^2$ after 5 h. Observation of the samples after EIS testing indicated that the number and size of corrosion pits on the coating deposited from the solution with a Ce^{3+} concentration of 0.1 M was less than the other coatings. Collectively, the results indicate that increasing the cerium concentration in the spray solution improved the corrosion performance of the coating up to 0.10 M after which the corrosion resistance degraded due to cracking of the film.

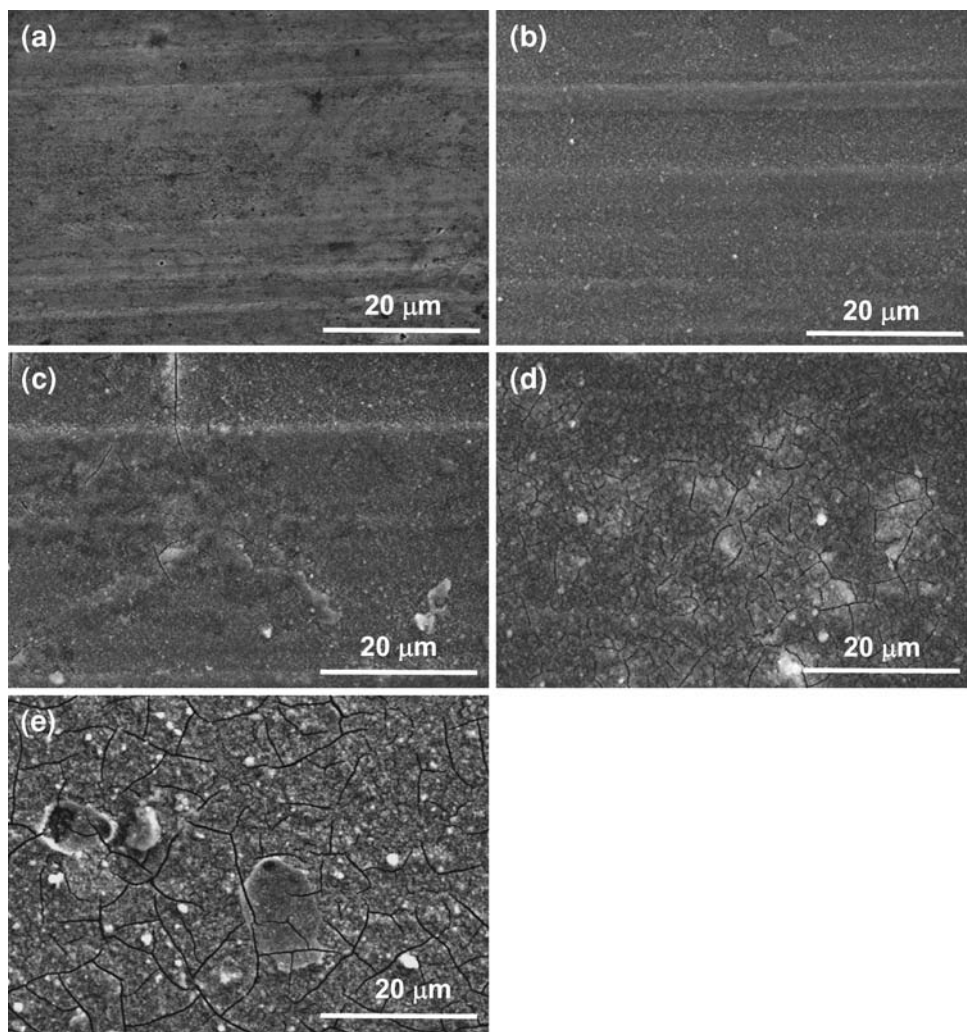
The concentration of Ce^{3+} in the spray solutions influenced not only surface morphology, but also the coating thickness. The surfaces of the coatings deposited from solutions with lower concentration (0.025 and 0.05 M) had nodules approximately 20 μm in diameter. No nodules were observed in the coatings deposited from solutions with higher Ce^{3+} concentration (0.075 and 0.1 M). The thickness of the coatings increased with increasing Ce^{3+} concentrations. The coating deposited from the solution with a Ce^{3+} concentration of 0.1 M demonstrated better corrosion resistance than other coatings based on the combination of impedance measured in EIS and surface appearance after 5 h of immersion in prohesion solution. For the coatings deposited from solutions with Ce^{3+} concentrations of 0.025 and 0.05 M, pitting corrosion is likely related to the inhomogeneous surfaces, which had nodules $\sim 20 \mu\text{m}$ in diameter. However, pitting corrosion was also observed for the coating deposited from the solution with a Ce^{3+} concentration of 0.075 M, which had a similar surface appearance to the coating deposited from the solution with a Ce^{3+} concentration of 0.1 M. The coating deposited from the solution with a Ce^{3+} concentration of 0.1 M was thicker than that of the coating deposited from a Ce^{3+} concentration of 0.075 M, which could be responsible for the improved corrosion resistance of the coating. However, the coating deposited from the solution with a higher concentration of Ce^{3+} , 0.125 M, had reduced the corrosion resistance due to extensive cracking.

3.3 Effect of H_2O_2 concentration in the spray solution

The concentration of H_2O_2 was varied from 0 to 1.2 M in coating solutions. Based on the results presented in Sects. 3.1 and 3.2, the concentration of Ce^{3+} was maintained at 0.1 M and the pH was adjusted to 2 using HCl.

Figure 7 shows the surface morphologies of coatings deposited from solutions with different concentrations of H_2O_2 . It is noted that cracks in the coatings became more prevalent with increasing H_2O_2 concentration. For example, the coating from 1.2 M solution had more cracks and

Fig. 7 Surface morphologies of CeCCs on Al 2024-T3 deposited from spray solutions with H₂O₂ concentrations of 0 M (a), 0.2 M (b), 0.4 M (c), 0.8 M (d), and 1.2 M (e)



defects than others as shown in Fig. 7e. The EDS results are plotted in Fig. 8, showing the measured amounts of Ce in the coatings deposited from solutions with different concentrations of H₂O₂. No Ce was detected by EDS in the coating deposited from the solution without H₂O₂ and the Ce concentrations in the coatings deposited from solutions with H₂O₂ concentrations of 0.2–1.2 M H₂O₂ increased as the H₂O₂ concentration in the coating solution increased. Thickness was measured by AES depth profile analysis confirmed that coatings deposited from solutions with higher H₂O₂ concentrations were thicker. Coating thickness increased from ~160 nm for a H₂O₂ concentration of 0.2 M to ~350 nm for H₂O₂ concentrations of 1.0 and 1.2 M.

In order to evaluate the effect of H₂O₂ concentration on corrosion resistance, Nyquist plots were prepared for different immersion times (Fig. 9). For the solution without any H₂O₂, no coating was deposited so the impedances were similar for all immersion times. Generally, higher H₂O₂ concentrations led to higher measured impedances in the

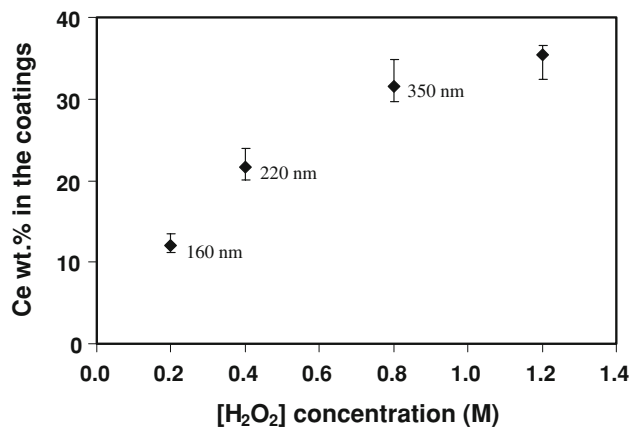


Fig. 8 Ce concentrations detected by EDS for CeCCs on Al alloy 2024-T3 deposited from spray solutions with different concentrations of H₂O₂ and the corresponding thickness measured by AES depth profiling analysis

coatings. The exception was that the coating deposited from the solution with a H₂O₂ concentration of 0.4 M had the highest impedance, more than $1.5 \times 10^5 \Omega \text{ cm}^2$, after 1 h.

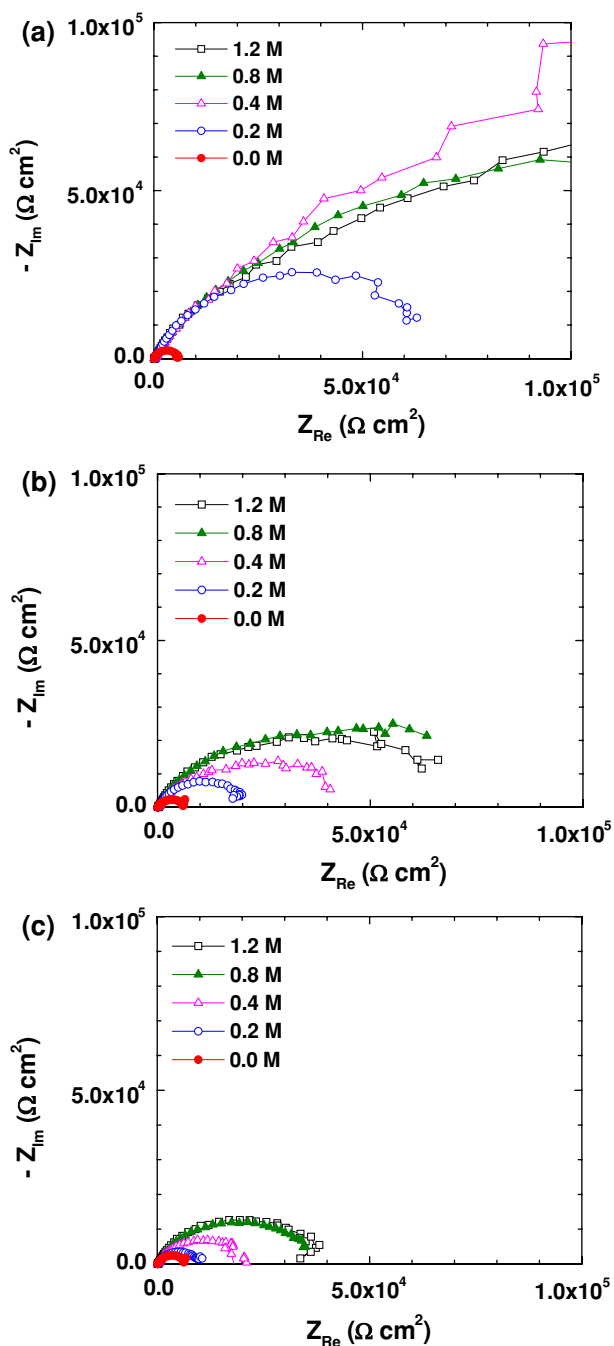


Fig. 9 Nyquist plots for CeCCs on Al alloy 2024-T3 deposited from spray solution with different concentrations of H_2O_2 after immersion in prohesion solution at $30\text{ }^\circ\text{C}$ for 1.0 h (a), 3.0 h (b), and 5.0 h (c)

However, after 3 and 5 h of immersion, coatings deposited from the solutions with H_2O_2 concentrations of the 0.8 and 1.2 M had higher impedance values, around $4.0 \times 10^4\ \Omega\ \text{cm}^2$. As expected, the coating deposited from the solution without H_2O_2 was covered with corrosion pits and tails after EIS testing. The number of corrosion pits and tails from the coating solution with 0.2 M H_2O_2 was less than the one deposited from a solution without H_2O_2 , but it still showed

significant corrosion. The coating deposited from the solution with an H_2O 0.4 M H_2O_2 exhibited better corrosion resistance than those deposited from the solution with 0.2 M and without H_2O_2 . The best corrosion resistance was demonstrated by the coating deposited from the solution with 0.8 M H_2O_2 , as the number of corrosion pits was less than that of the coating deposited from solution with an H_2O_2 concentration of 1.2 M.

4 Conclusions

The effects of changes in pH, cerium concentration, and concentration of H_2O_2 in spray solution used to deposit CeCCs were investigated. Results from the studies include:

1. The pH of spray solutions had no measurable effect on the amount of Ce detected in the coating, indicating that pH had no effect on coating thickness. The electrochemical impedance and corrosion resistance of the coatings deposited from solutions with pH 2.0 and 2.5 were higher than those deposited from solutions with pH 1.0 and 1.5 in prohesion solution. The coating deposited from solution with pH 2.0 had fewer corrosion pits than others after impedance testing.
2. The amount of Ce detected in the coating increased with increasing Ce^{3+} concentration in the spray solutions within the range of 0.025 to 0.125 M. The coating deposited from the solution with a 0.1 M Ce^{3+} exhibited the best corrosion resistance as measured by the number of pits present after impedance testing.
3. Increasing the concentration of H_2O_2 up to 1.2 M in the spray solution increased the amount of Ce in the coating. The coatings deposited from solution with 0.8 M H_2O_2 had higher impedance and fewer corrosion pits than others after impedance testing.

Based on analysis of the results, solution pH, Ce^{3+} concentration, and H_2O_2 concentration all impacted coating deposition and performance. At pH values below 2.0 cracks and holes in the coating resulted in lower impedance and more corrosion pits that were 350 nm thick. Similarly, if the Ce^{3+} concentration was above 0.1 M or the H_2O_2 concentration was above 0.8 M the coating had lower impedance and corrosion resistance, in both cases the films were over 350 nm in thickness. The best combination of processing parameters for optimal coating performance was deposition from a solution with pH = 2.0, $[\text{Ce}^{3+}] = 0.100\ \text{M}$ and $[\text{H}_2\text{O}_2] = 0.8\ \text{M}$ that was about 350 nm thick. This combination of processing parameters provides at balance of coating thickness, morphology, and impedance, which results in the best corrosion resistance.

Acknowledgments This work was funded through the Strategic Environmental Research and Development Program under contract 912HQ-06-C-0030. The authors would like to acknowledge the technical guidance and support of Charles Pellerin and Bruce Sartwell at SERDP and Donna Ballard at the Air Force Research Laboratory. We also appreciate the assistance from Clarissa Wisner (SEM) and Jeff Wight (AES) at the Materials Research Center, Missouri University of Science and Technology.

References

1. Buchheit RG, Grant RP, Hlava PF, McKenzie B, Zender GL (1997) *J Electrochem Soc* 144:2621–2628
2. Buchheit RG (1995) *J Electrochem Soc* 142:3994–3996
3. Hughes AE, Taylor RJ, Hinton BRW (1997) *Surf Interface Anal* 25:223–234
4. Zhao J, Xia L, Sehgal A, Lu D, McCreery RL, Frankel GS (2001) *Surf Coat Technol* 140:51–57
5. Brown GM, Kobayashi K (2001) *J Electrochem Soc* 148:B457–B466
6. Vasquez MJ, Halada GP, Clayton CR, Longtin JP (2002) *Surf Interface Anal* 33:607–616
7. Campestrini P, Terryn H, Vereecken J, de Wit JHW (2004) *J Electrochem Soc* 151:B359–B369
8. Chidambaram D, Clayton CR, Halada GP, Kendig NW (2004) *J Electrochem Soc* 151:B605–B612
9. Chidambaram D, Clayton CR, Kendig NW, Halada GP (2004) *J Electrochem Soc* 151:B613–B620
10. Hinton BRW, Arnott DR, Ryan NE (1984) *Mater Forum* 7:211
11. Hinton BRW, Arnott DR, Ryan NE (1986) *Mater Forum* 9:162
12. Hinton BRW, Alloy J (1992) *Compounds* 180:15–25
13. Mansfeld F, Wang Y (1995) *Mater Sci Eng A* 198:51–61
14. Fahrenholtz WG, O’Keefe MJ, Zhou HF, Grant JT (2002) *Surf Coat Technol* 155:208–213
15. Johnson BY, Edington J, O’Keefe MJ (2003) *Mater Sci Eng A* 361:225–231
16. Rivera BF, Johnson BY, O’Keefe MJ, Fahrenholtz WG (2004) *Surf Coat Technol* 176:349–356
17. Johnson BY, Edington J, Williams A, O’Keefe MJ (2005) *Mater Charact* 54:41–48
18. Wang C, Jiang F, Wang F (2004) *Corrosion* 60:237–243
19. Hughes AE, Gorman JD, Miller PR, Sexton BA, Paterson PJK, Taylor RJ (2004) *Surf Interface Anal* 36:290–303
20. Palomino LEM, Aoki IV, de Melo HG (2006) *Electrochim Acta* 51:5943–5953
21. Jones P, Yu P, Pinc WR, O’Keefe MJ, Fahrenholtz W, O’Keefe TJ (2008) *Int J Appl Ceram Technol* 5(1):63–73
22. You S, Jones P, Padwal A, Yu P, O’Keefe M, Fahrenholtz W, O’Keefe T (2007) *Mater Lett* 61(17):3778–3782
23. Geng S, Pinc W, Yu P, Jones P, O’Keefe M, Fahrenholtz W, O’Keefe T (2007) *J Appl Surf Finish* 2(4):276–282
24. Pinc WR, Yu P, O’Keefe M, Fahrenholtz W (2009) *Surf Coat Technol* 203(23):3533–3540
25. Pinc WR, Geng S, O’Keefe M, Fahrenholtz W, O’Keefe T (2009) *Appl Surf Sci* 255(7):4061–4065
26. Jones PS, Yu P, Pinc WR, O’Keefe MJ, Fahrenholtz WG, O’Keefe TJ (2007) *Int J Appl Ceram Technol* 5(1):63–73
27. Scholes FH, Soste C, Hughes AE, Hardin SG, Curtis PR (2006) *Appl Surf Sci* 253(4):1770–1780
28. Hayes SA, Yu P, O’Keefe TJ, O’Keefe MJ, Stoffer JO (2002) *J Electrochem Soc* 149(12):623–630
29. Edington J, O’Keefe M, O’Keefe T (2006) *Surf Coat Technol* 200(20/21):5733–5737